2024 European Control Conference (ECC)
June 25-28, 2024. Stockholm, Sweden

CAVs platoons under nonlinear spacing policy and heterogeneous communication delays as a formation control problem

Gennaro Nicola Bifulco[1], Angelo Coppola[1], Aniello Mungiello[2], Alberto Petrillo[2] and Stefania Santini[2]

Abstract— **This paper solves the platoon control of nonlinear connected autonomous vehicles under variable spacing policy as a formation problem. The main aim is to guarantee that each vehicle, despite wireless communication impairments, moves according to the imposed speed profile while following the desired spacing, adaptable to different traffic conditions. To this end, we first design a novel full-range nonlinear spacing policy and then, by leveraging formation control theory, a distributed controller ensuring CAVs platoon variable formation, despite the presence of heterogeneous communication time-delay. By exploiting the Lyapunov-Krasovskii approach, we derive a delay-dependent stability condition that, expressed as a set of feasible Linear Matrix Inequalities, allows tuning control gains. Simulation results, carried out via MiTraS platform, disclose the effectiveness of the proposed solution.**

I. INTRODUCTION

Vehicle platooning composed of Connected and Automated Vehicles (CAVs) has been extensively studied since it is expected to mitigate traffic congestion while increasing road safety and traffic throughput [1], [2]. A key element of platooning control strategies is the spacing policy. Its choice is not trivial: limited inter-vehicle distance may enhance traffic throughput but compromises safety; on the other hand, the optimization of traffic flow requires spacing policy to be adaptable to the prevailing traffic conditions. The policies employed the most in the technical literature, the Constant Spacing (CS) and the Constant Time Headway/Gap (CTH/CTG) [3], are not flexible enough, especially in rapidly changing speed situations, and they lead to a non-optimal utilization of road in term of throughput [4]. To overcome these limitations, many nonlinear spacing policies have been proposed, although their usage for platooning applications has received less attention. In this direction, a quadratic spacing policy is employed in [5], where, by leveraging geometric control theory, a decentralized predecessor follower nonlinear state feedback control is suggested to let linear CAVs platoon tracking a desired behaviour. Considering, instead, the specific case of heterogeneous CAVs platoon subject to actuator faults, input quantization and dead-zone nonlinearities, [6] introduces an improved quadratic spacing policy based on vehicle speed, braking capacity and lower bound of fault factor. Then, an adaptive fault-tolerant control, combined with an adaptive radial basis function neural network for the estimation of nonlinear vector field, is proposed for ensuring the tracking of the variable spacing.

All the aforementioned works design platooning controller for variable spacing policy under some restrictive assumptions, such as perfect wireless communication, linear/simplified vehicle dynamics and large inter-vehicle distance, which can lead to platoon performance degradation in practice. To deal with the presence of Vehicle-to-Vehicle (V2V) homogeneous communication delays, [7] proposes a delayed consensus-based control strategy for a platoon of homogeneous linear second-order CAVs under the quadratic human policy developed in [8] and subject to acceleration saturation. More recently, to improve the platoon safety, [9] proposes a variable spacing policy which adapts the inter-vehicle headway based on the actual road friction and designs a back-stepping control to ensure its maintenance. However, the main drawback of such approach is related to its applicability in real-world due to the necessity of estimating the road friction, which is a complex and error-prone operation [10]. Again, the platoon control problem for heterogeneous linear CAVs sharing information over a realistic V2V communication network has been addressed and solved in [11] via integral sliding mode controller to ensure the leader-tracking under quadratic human spacing policies.

However, it is worth noting that all the aforementioned spacing policies do not simultaneously guarantee a safe response in the full speed range and a maximization of the traffic throughput. To this end, [12] proposes a full-range nonlinear spacing policy, adaptable to both urban and highway scenarios (i.e. low and high speeds), but for the simpler case of the CACC of linear homogeneous autonomous vehicles sharing information over ideal V2V network.

The above discussion highlights how it is crucial, with the purpose of optimizing the traffic flow throughput, choosing and explicitly taking into account innovative and more effective spacing policies when designing platooning control strategies. This task becomes more challenging when considering vehicle dynamic nonlinearities, V2V time-varying communication delays and external disturbances. In this case, the control objective is to guarantee that the CAVs platoon adapts its own formation to the current traffic situation while ensuring resilience and robustness to communication time-delay and vehicles nonlinearities. In this perspective, the aim of this work is twofold. Firstly, we design a novel nonlinear

This work was founded by the Ministero Università e Ricerca (MUR), Italy, through the PNRR project Centro Nazionale per la Mobilita Sostenibile (CNMS) CUP E63C22000930007

Authors are in alphabetic order

[1] Department of Architectural and Environmental Engineering (DICEA), University of Naples Federico II, Naples 80125, Italy, e-mail: {gennaro.bifulco,angelo.coppola}@unina.it

[2] Department of Information Technology and Electrical Engineering (DIETI), University of Naples Federico II, Naples 80125, Italy, e-mail:{aniello.mungiello, alberto.petrillo, stefania.santini}@unina.it

spacing policy covering the full speed range so to ensure a smooth transition between fixed distance at standstill and the desired time gap at high speeds. Then, in order to follow the desired variable spacing policy while guaranteeing a robust and resilient tracking of a desired speed profile, the CAVs platoon control is recast as a formation control problem. A robust delayed distributed controller is, hence, proposed to ensure that CAVs platoon safely moves in formation. Simulation results, carried out via MiTraS platform [13], confirm the effectiveness of the theoretical derivation and discloses the advantages of the proposed approach.

II. Platoon formation Control under nonlinear variable spacing policy

Consider a platoon composed of N heterogeneous CAVs plus a leader, indexed with 0, moving as a string along a straight road. The aim is to design a robust distributed formation controller ensuring that each CAV adheres to the prescribed behavior set by the leader, while maintaining a desired variable nonlinear inter-vehicle spacing.

A. Nonlinear Heterogeneous Platoon Dynamics

The longitudinal dynamics of each CAV i ($\forall i = 1,...N$) is described by its drivetrain dynamics [14]:

$$\begin{aligned} \dot{p}_i(t) &= v_i(t), \\ \dot{v}_i(t) &= \frac{\eta_i}{R_i m_i} u_i(t, \tau_{ij}(t)) - g sin(\theta(t)) - g f_{r,i} cos(\theta(t)) \\ &\quad - \frac{0.5}{m_i} \rho C_{D,i} A_{f,i} v_i^2(t), \end{aligned} \tag{1}$$

where $p_i(t)$ $[m]$ and $v_i(t)$ $[m/s]$ are the position and the speed; m_i $[kg]$ is the vehicle mass while η_i is its drivetrain mechanical efficiency; R_i $[m]$ is the wheel radius; $f_{r,i}$ is the rolling resistance coefficient; $C_{D,i}$ and $A_{f,i}$ $[m^2]$ are the drag coefficient and the frontal area; ρ $[kg/m^3]$ is the air density; g $[m/s^2]$ is the gravity acceleration; $\theta(t)$ $[rad]$ is the road slope; $u_i(t, \tau_{ij}(t))$ $[Nm]$ is the driving/braking torque control input. Since CAVs share information via a non-ideal communication network, each link connecting vehicles i and j is affected by a time-varying heterogeneous communication delay $\tau_{ij}(t)$, whose value depends on the actual conditions/impairments of the communication channel.

Assumption 1: According to [15], V2V communication time-delay $\tau_{ij}(t)$ is assumed to be bounded and slowly-varying, i.e. $\tau_{ij}(t) \leq \tau_{ij}^\star$ and $\dot{\tau}_{ij}(t) \leq \mu_{ij} \in [0,1[$.

Indicating with $x_i(t) = [p_i(t), v_i(t)]^\top \in \mathbb{R}^{2\times 1}$ the i-th vehicle state vector, the nonlinear dynamic in (1) can be recast as:

$$\dot{x}_i(t) = \begin{bmatrix} v_i(t) \\ \varphi_i(v_i(t)) \end{bmatrix} + \begin{bmatrix} 0 \\ b_i \end{bmatrix} u_i(t, \tau_{ij}(t)) \tag{2}$$

where $b_i = \eta_i/(m_i R_i)$ while $\varphi_i(v_i(t)) \in \mathbb{R}$ is a continuously differentiable and bounded nonlinear vector field, defined as: $\varphi_i(v_i(t)) = -g sin(\theta(t)) - g f_{r,i} cos(\theta(t)) - \frac{0.5}{m_i} \rho C_{D,i} A_{f,i} v_i^2(t)$.
The leader dynamics imposing the reference behaviour for the whole vehicle platoon, can be, instead, described by the following nonlinear autonomous system:

$$\dot{x}_0(t) = \begin{bmatrix} v_0(t) \\ \varphi_0(v_0(t)) \end{bmatrix}. \tag{3}$$

where $x_0(t) = [p_0(t)\ v_0(t)]^\top$, being $p_0(t)$ $[m] \in \mathbb{R}[m/s]$ and $v_0(t) \in \mathbb{R}$ the position and the speed of the leading vehicle.

B. Communication Network

The communication among CAVs is modeled as a directed graph $\mathscr{G}_N = (\mathscr{V}_\mathscr{N}, \mathscr{E}_\mathscr{N}, \mathscr{A})$ where $\mathscr{V}_N$ is the set of N vehicles while $\mathscr{E}_N$ is the set of communication links. The adjacency matrix $\mathscr{A}[\alpha_{ij}]_{N\times N}$ describes the communication graph topology with elements such that: $\alpha_{ij} = 1$ if vehicle j receives information from vehicle i (but not necessarily *viceversa*), $\alpha_{ij} = 0$ otherwise. Accordingly, after introducing the in-degree matrix $\mathscr{D} = diag\{d_1, d_2, \dots, d_N\}$, with $d_i = \sum_{j\in\mathscr{V}} \alpha_{ij}$ (i.e. the number of vehicles communicating with i), we define the Laplacian matrix of the digraph $\mathscr{G}_N$ as $\mathscr{L} = \mathscr{D} - \mathscr{A}$. Taking into consideration that the leader is considered as an additional agent, labeled with the index 0, the whole vehicular network topology is modelled via an augmented directed graph $\mathscr{G}_{N+1}$ satisfying the following assumption.

Assumption 2: $\mathscr{G}_{N+1}$, contains a directed spanning tree with the leader node as root, i.e. the information about the leader is available for each CAV i, directly or indirectly [16].

C. Design of Nonlinear Variable Spacing Policy

The proposed spacing policy is formulated considering the different driving conditions that platoons may encounter, i.e. urban, freeway and motorway. Since urban conditions require avoiding too high inter-vehicle distances while extra-urban scenarios, both freeway and motorway, require higher inter-vehicle distances due to high travelling speed, the spacing policy should be designed as a variable function ensuring the right trade-off between traffic throughput increasing and vehicles safety in all driving scenarios. Accordingly, indicating with $d_{ref,i}(v_i(t))$ the desired inter-vehicle distance between consecutive vehicles, based on [17], we propose the following full-range nonlinear variable spacing policy between vehicle i and the communicating vehicle j:

$$\begin{aligned} d_{ref,ij}(t) &= (i-j) d_{ref,i}(v_i(t)) \\ &= (i-j)\Big\{ d_{st} + v_i(t) h + M[1 - exp(-\frac{v_i(t)}{\gamma})] \Big\}, \end{aligned} \tag{4}$$

where d_{st} $[m]$ is the standstill distance; $v_i(t)$ $[m/s]$ is the speed of vehicle i; h $[s]$ is the constant time-gap distance; M and γ are parameters to be properly tuned via the optimization procedure described in the following.

1) Spacing Policy Parameters Tuning: The optimization procedure finds the parameters M and γ in (4) such that, in the whole vehicles speed range, the variable spacing policy $d_{ref,i}(v_i(t))$ ensures the following objectives: 1) increasing of the traffic throughput; 2) ensuring vehicle safety.
The design starts dividing the speed range according to

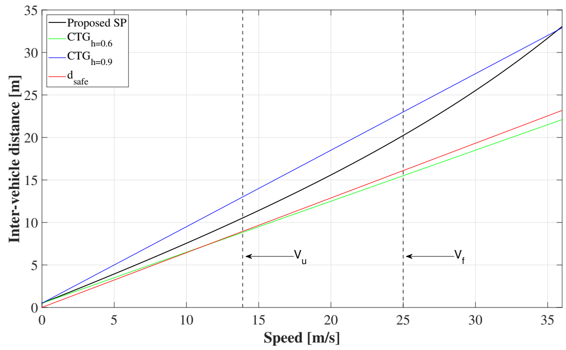

Fig. 1: Full-range spacing policy (blank line) against minimal safe distance (red line) and two CTG (blue and green lines).

the driving scenario, namely: urban, freeway and motorway, which have $V_0 = 0$ $[m/s]$, $V_u = 13.89$ $[m/s]$, $V_f = 25$ $[m/s]$ and $V_m = 36$ $[m/s]$ as speed limits, respectively. To take into account the objective of traffic throughput, we set $d_{st} = 0.5$ $[m]$ and $h = 0.6$ $[s]$, i.e. lower than the typical ones [3]. Then, we define the reference values of inter-vehicle distance at range speed boundaries as: $d_{ref,i}(V_0) = d_{st} + 0.60V_0$ $[m]$ and $d_{ref,i}(V_m) = d_{st} + 0.90V_m$ $[m]$. Moreover, we compute the minimum critical distance as $d_{safe,i}(t) = (\tau_{ac} + \frac{B_{max}}{2J_{max}})v_i(t) - \frac{B_{max}^3}{24J_{max}^2}$ $[m]$ [12], where $\tau_{ac} = 0.2$ $[s]$ is the delay of actuator response; $B_{max} = 4$ $[m/s^2]$ and $J_{max} = 5.5$ $[m/s^3]$ are the maximum braking deceleration and jerk (also considering comfort conditions).

To achieve the objectives 1)-2), parameters M and γ are chosen as the solution of the following optimization problem:

$$\min_{M,\gamma} d_{ref,i}(v_i(t)) \tag{5}$$

subject to:

$$\begin{array}{cc} d_{ref,i}(V_0) = d_{st} + 0.60V_0 & d_{ref,i}(V_m) = d_{st} + 0.90V_m \\ 0 \leq v_i(t) \leq 36 & d_{ref,i}(v_i(t)) \geq d_{safe,i}(v_i(t)). \end{array}$$

The solution, obtained via the Matlab Optimization Toolbox, provides the following results: $M = -1.5976$ and $\gamma = -21.0172$. The resulting $d_{ref,i}(v_i(t))$ is reported in Figure 1.

Assumption 3: Due to vehicle physical constraint, $d_{ref,ij}(t)$ is a bounded piecewise-continuously differentiable function $\forall i, j \in \mathscr{V}_{N+1}$.

D. Platoon Control as a Formation Problem

The platoon control is here formulated as the following second-order nonlinear formation problem.

Problem 1: (Heterogeneous Nonlinear Platoon Formation Control Problem). *Given the heterogeneous nonlinear vehicle model as in* (1)*, design the distributed control input* $u_i(t)$ $(\forall i \in \mathscr{V}_N)$ *such that vehicle* i *tracks the reference behaviour imposed by the leader in* (3) *while maintaining the reference gap* $d_{ref,ij}(t)$ *w.r.t. the neighbors* j*, i.e.:*

$$\begin{aligned} &\lim_{t\to\infty} \|p_i(t) - p_j(t) - d_{ref,ij}(t)\| = 0, \\ &\lim_{t\to\infty} \|v_i(t) - v_0(t) - \dot{d}_{ref,ij}(t)\| = 0, \end{aligned} \tag{6}$$

despite the presence of heterogeneous communication time-varying delays $\tau_{ij}(t)$ $(\forall (i,j) \in \mathscr{E}_{N+1})$ *affecting the communication network.*

III. Design of Distributed Formation Control

Define, for each CAV i, the error formation w.r.t. the leader as

$$e_i(t) = \begin{bmatrix} e_{p,i} \\ e_{v,i} \end{bmatrix} = \begin{bmatrix} p_i(t) - p_0(t) - d_{ref,i0}(t) \\ v_i(t) - v_0(t) - \dot{d}_{ref,i0}(t) \end{bmatrix}. \tag{7}$$

To solve Problem 1, we propose the following distributed formation control protocol:

$$u_i(t, \tau_{ij}(t)) = b_i^{-1}\Big(u_{i,net}(e_i(t), e_j(t), t, \tau_{ij}(t)) + \nu_i(t)\Big), \tag{8}$$

where $u_{i,net}(e_i(t), e_j(t), t, \tau_{ij}(t))$ is the networked control action that weights the outdated information shared among vehicles via the V2V communication paradigm while $\nu_i(t)$ is the local feed-forward control action which is used to compensate the variation of the formation signal. Specifically, the networked control action is designed as:

$$\begin{aligned} &u_{i,net}(e_i(t), e_j(t), t, \tau_{ij}(t)) = \\ &\quad - \sum_{j=0}^{N} \alpha_{ij}\kappa_{ij}(p_i(t - \tau_{ij}(t)) - p_j(t - \tau_{ij}(t)) - d_{ref,ij}(t - \tau_{ij}(t))) \\ &\quad - \sum_{j=0}^{N} \alpha_{ij}\beta_{ij}(v_i(t - \tau_{ij}(t)) - v_j(t - \tau_{ij}(t)) - \dot{d}_{ref,ij}(t - \tau_{ij}(t))), \end{aligned} \tag{9}$$

being $\kappa_{ij} \in \mathbb{R}$ and $\beta_{ij} \in \mathbb{R}$ $(\forall i, j \in \mathscr{V}_{N+1})$ the control gains to be properly tuned. The local feed-forward control action is, instead, selected as $\nu_i(t) = \ddot{d}_{ref,i0}(t)$.

A. Closed-loop system

Given the i-th CAV dynamics as in (2) and the ones of the leader as in (3), by differentiating the formation error in (7), the closed-loop dynamics for vehicle i can be derived as:

$$\dot{e}_i(t) = \begin{bmatrix} \dot{e}_{p,i}(t) \\ \dot{e}_{v,i}(t) \end{bmatrix} = \begin{bmatrix} e_{v,i}(t) \\ \varphi_i(v_i(t)) - \varphi_0(v_0(t)) + b_i u_i(t) - \ddot{d}_{ref,i0}(t) \end{bmatrix}. \tag{10}$$

Substituting (8) in (10), given the error definition in (7), we derive the closed-loop dynamics for the i-th vehicle as:

$$\begin{aligned} \dot{e}_i(t) =& \bar{\varphi}_i(e_{v,i}(t)) + \alpha_{i0}A_{i0}e_i(t - \tau_{i0}(t)) \\ &+ \sum_{j=1}^{N} \alpha_{ij}A_{ij}(e_i(t - \tau_{ij}(t)) - e_j(t - \tau_{ij}(t))), \end{aligned} \tag{11}$$

where

$$\begin{aligned} &\bar{\varphi}_i(e_{v,i}(t)) = \begin{bmatrix} e_{vi}(t) \\ \varphi_i(v_i(t)) - \varphi_0(v_0(t)) \end{bmatrix}, \\ &A_{i0} = \begin{bmatrix} 0 & 0 \\ -\kappa_{i0} & -\beta_{i0} \end{bmatrix} \; A_{ij} = \begin{bmatrix} 0 & 0 \\ -\kappa_{ij} & -\beta_{ij} \end{bmatrix}. \end{aligned} \tag{12}$$

By exploiting a more compact notation [18], delays $\tau_{ij}(t)$ can be represented as elements of the following delay sets: $\sigma_p(t) \in \{\tau_{ij}(t) : i, j = 1, 2, ..., N, i \neq j)\}$ for $p = 1, 2, ..., m$ with $m \leq N(N-1)$; $\tau_l(t) \in \{\tau_{i0}(t) : i = 1, 2, ..., N,\}$ for $l = 1, 2, ..., q$ with $q \leq N$. Accordingly, by defining the global error formation vector $\tilde{x} = [e_1^\top(t)\; e_2^\top(t) \;\cdots\; e_N^\top(t)]^\top$, the overall closed-loop delayed vehicular network dynamics can be derived as:

$$\dot{\tilde{x}}(t) = \psi(\tilde{x}(t)) + \sum_{l=1}^{q} A_{(l,\tau)}\tilde{x}(t-\tau_l(t)) + \sum_{p=1}^{m} A_{(p,\sigma)}\tilde{x}(t-\sigma_p(t)), \tag{13}$$

where

$$\psi(\tilde{x}(t)) = [\bar{\varphi}_1^\top(e_{v,1}(t))\ \bar{\varphi}_2^\top(e_{v,2}(t)); \cdots ; \bar{\varphi}_N^\top(e_{v,N}(t))]^\top \in \mathbb{R}^{2N\times 1}, \tag{14}$$

$$A_{(l,\tau)} = \begin{bmatrix} \mathscr{A}_{1,1} & 0^{2\times 2} & \cdots & 0^{2\times 2} \\ 0^{2\times 2} & \mathscr{A}_{2,2} & \cdots & \vdots \\ \vdots & \vdots & \ddots & \vdots \\ 0^{2\times 2} & \cdots & \cdots & \mathscr{A}_{N,N} \end{bmatrix} \in \mathbb{R}^{2N\times 2N}, \tag{15}$$

with diagonal blocks such that ($i = 1,\dots,N$; $l = 1,\dots,q$)

$$\mathscr{A}_{i,i}^{2\times 2} = \begin{cases} A_{i0} & i = l, \tau_l(\cdot) = \tau_{il}(\cdot), \\ 0^{2\times 2} & i \neq l, \tau_l(\cdot) \neq \tau_{il}(\cdot), \end{cases} \tag{16}$$

being A_{i0} as in (12). Matrices $A_{(p,\sigma)} \in \mathbb{R}^{2N\times 2N}$ ($p = 1,\cdots,m$) in (13) are block matrices such that each block (referred for the sake of clarity as $\mathscr{A}_{p(r,q)} \in \mathbb{R}^{2\times 2}$) is given as:

$$\mathscr{A}_{p(r,q)} = \begin{cases} A_{ij} & i \neq j \quad \text{if} \quad \sigma_p(\cdot) = \tau_{ij}(\cdot), r = q = i \\ -A_{ij} & i \neq j \quad \text{if} \quad \sigma_p(\cdot) = \tau_{ij}(\cdot), r = i, q = j \\ 0^{2\times 2} & \text{otherwise} \end{cases} \tag{17}$$

being $r,q = \{1,2,\cdots N\}$ and A_{ij} as in (12). Given the definition of the closed-loop system in (13), since each vector field $\bar{\varphi}_i(\bar{v}_i(t))$ is continuous, differentiable and bounded, i.e. a Lipschitz function, the following condition holds.

Condition 1: [19] There exist constants ω_i ($\forall i = 1,\cdots,N$) such that for any vectors $x_i(t), x_0(t)$, the vector fields $\bar{\varphi}_i(.)$ satisfy the condition:

$$(x_i(t) - x_0(t))^\top \left(\bar{\varphi}_i(x_i(t)) - \bar{\varphi}_0(x_0(t))\right) \leq \omega_i (x_i(t) - x_0(t))^\top (x_i(t) - x_0(t)). \tag{18}$$

IV. Stability Analysis

The stability of the CAVs platoon under the action of the proposed distributed formation control is ensured by the following delay-dependent theorem which allows the proper tuning of the control gains.

Theorem 1: Consider the closed-loop vehicular network dynamics as in (13). Let Assumptions 1-2-3 and Condition 1 hold. Given the maximum allowable delay margin $\tau^\star$, if there exist symmetric positive definite matrices $Q_{(l,\tau)}, Q_{(p,\sigma)}, W_{(l,\tau)}, W_{(p,\sigma)} \in \mathbb{R}^{2N\times 2N}$ ($l = 1,2,\cdots,q$ and $p = 1,2,\cdots,m$) such that the following LMI holds:

$$\Phi + \sum_{l=1}^{q} Q_{(l,\tau)} + \sum_{p=1}^{m} Q_{(p,\sigma)} + (m+q)\tau^\star \Big(\sum_{l=1}^{q} W_{(l,\tau)} + \sum_{p=1}^{m} W_{(p,\sigma)} \Big) < 0 \tag{19}$$

with $\Phi = \text{diag}(\Psi_1,\cdots,\Psi_N) + \sum_{l=1}^{q} A_{(l,\tau)} + \sum_{p=1}^{m} A_{(p,\sigma)} \in \mathbb{R}^{2N\times 2N}$, being $\Psi_i = \begin{bmatrix} 0 & 1 \\ 0 & \omega_i \end{bmatrix}$ ($i = 1,\dots,N$), as well as $A_{(l,\tau)}$ and $A_{(p,\sigma)}$ defined as in (15) and (17), respectively, then the platoon formation control under nonlinear variable spacing policy is achieved.

Proof: Consider the following Lyapunov-Krasovskii functional

$$V(\tilde{x}(t)) = V_1(\tilde{x}(t)) + V_2(\tilde{x}(t)) + V_3(\tilde{x}(t)), \tag{20}$$

being

$$V_1(\tilde{x}(t)) = \frac{1}{2}\tilde{x}^\top(t)\tilde{x}(t), \tag{21a}$$

$$V_2(\tilde{x}(t)) = \sum_{l=1}^{q} \int_{t-\tau_l(t)}^{t} \tilde{x}^\top(s) Q_{(l,\tau)} \tilde{x}(s) ds + \sum_{p=1}^{m} \int_{t-\sigma_p(t)}^{t} \tilde{x}^\top(s) Q_{(p,\sigma)} \tilde{x}(s) ds, \tag{21b}$$

$$V_3(\tilde{x}(t)) = \sum_{l=1}^{q} \int_{-\tau_l^\star}^{0} \int_{t+\theta}^{t} \tilde{x}^\top(s) W_{(l,\tau)} \tilde{x}(s) ds d\theta, + \sum_{p=1}^{m} \int_{-\sigma_p^\star}^{0} \int_{t+\theta}^{t} \tilde{x}^\top(s) W_{(p,\sigma)} \tilde{x}(s) ds d\theta. \tag{21c}$$

Differentiating $V_1(\tilde{x}(t))$ in (21a) along the trajectories of the closed-loop system (13) we have:

$$\dot{V}_1(\tilde{x}(t)) = \tilde{x}^\top(t)\psi(\tilde{x}(t)) + \tilde{x}^\top(t) \sum_{l=1}^{q} A_{(l,\tau)}\tilde{x}(t-\tau_l(t)) + \tilde{x}^\top(t) \sum_{p=1}^{m} A_{(p,\sigma)}\tilde{x}(t-\sigma_p(t)). \tag{22}$$

Focusing on the non linear vector field (14) and considering the expression of its elements as in (12), under Condition 1, the term $\tilde{x}^\top(t)\psi(\tilde{x}(t))$ in (22) is such that the following relation holds:

$$\tilde{x}^\top(t)\psi(\tilde{x}(t)) = \sum_{i=1}^{N} e_i^\top(t)\bar{\varphi}_i(e_{v,i}(t)) = \sum_{i=1}^{N} e_{p,i}(t)e_{v,i}(t) + e_{v,i}(t)\varphi_i(e_{v,i}(t)) \leq \sum_{i=1}^{N} e_{p,i}(t)e_{v,i}(t) + \omega_i e_{v,i}^2(t) \leq \tilde{x}^\top(t)\Psi\tilde{x}(t), \tag{23}$$

where $\Psi \in \mathbb{R}^{2N\times 2N} = \text{diag}(\Psi_1,\ \Psi_2,\cdots,\Psi_N)$ with $\Psi_i = [0\ \ 1; 0\ \ \omega_i] \in \mathbb{R}^{2\times 2}$. Then, by also applying the Newton-Leibiniz formula [15], i.e. $\tilde{x}(t-\tau(t)) = \tilde{x}(t) - \int_{t-\tau(t)}^{t} \dot{\tilde{x}}(s)ds$, we can recast (22) as:

$$\dot{V}_1(\tilde{x}(t)) \leq \tilde{x}^\top(t)\Phi\tilde{x}(t) - \tilde{x}^\top(t) \sum_{l=1}^{q} A_{(l,\tau)} \int_{t-\tau_l(t)}^{t} \dot{\tilde{x}}(s)ds - \tilde{x}^\top(t) \sum_{p=1}^{m} A_{(p,\sigma)} \int_{t-\sigma_p(t)}^{t} \dot{\tilde{x}}(s)ds, \tag{24}$$

where $\Phi = \Psi + \sum_{l=1}^{q} A_{(l,\tau)} + \sum_{p=1}^{m} A_{(p,\sigma)} \in \mathbb{R}^{2N\times 2N}$.
By differentiating $V_2(\tilde{x}(t))$ in (21b), under Assumption 1, it yields:

$$\dot{V}_2(\tilde{x}(t)) \leq \tilde{x}^\top(t) \sum_{l=1}^{q} Q_{(l,\tau)}\tilde{x}(t) + \tilde{x}^\top(t) \sum_{p=1}^{m} Q_{(p,\sigma)}\tilde{x}(t) - \sum_{l=1}^{q} \tilde{x}^\top(t-\tau_l(t)) Q_{(l,\tau)} (1-\mu_l) \tilde{x}(t-\tau_l(t)) - \sum_{p=1}^{m} \tilde{x}^\top(t-\sigma_p(t)) Q_{(p,\sigma)} (1-\mu_p) \tilde{x}(t-\sigma_p(t)). \tag{25}$$

Moreover, we differentiate $V_3(\tilde{x}(t))$ in (21c). Under Assumption 1, by exploiting Jensen inequality [15], it holds:

$$\begin{aligned}\dot{V}_3(\tilde{x}(t)) \leq & \tilde{x}^\top(t)\Big(\sum_{l=1}^{q}\tau_l^\star W_{(l,\tau)}\Big)\tilde{x}(t)+\tilde{x}^\top(t)\Big(\sum_{p=1}^{m}\sigma_l^\star W_{(p,\sigma)}\Big)\tilde{x}(t)\\ &-\sum_{l=1}^{q}\Big(\int_{t-\tau_l(t)}^{t}\tilde{x}(s)ds\Big)^\top W_{(l,\tau)}\Big(\int_{t-\tau_l(t)}^{t}\tilde{x}(s)ds\Big)\\ &-\sum_{p=1}^{m}\Big(\int_{t-\sigma_p(t)}^{t}\tilde{x}(s)ds\Big)^\top W_{(p,\sigma)}\Big(\int_{t-\sigma_p(t)}^{t}\tilde{x}(s)ds\Big).\end{aligned} \tag{26}$$

Now, introduce the maximum delay upper bound $\tau^\star = \max_{l,p}\{\tau_l^\star, \sigma_p^\star\}$ and use the free matrices method [20]:

$$\Big(\int_{t-\tau_l(t)}^{t}\dot{\tilde{x}}(s)ds\Big)^\top G_{(l,\tau)}^\top \times \Big[\tilde{x}(t)-\tilde{x}(t-\tau_l(t))-\int_{t-\tau_l(t)}^{t}\dot{\tilde{x}}(s)ds\Big]=0, \tag{27}$$

$$\Big(\int_{t-\sigma_p(t)}^{t}\dot{\tilde{x}}(s)ds\Big)^\top G_{(p,\sigma)}^\top \times \Big[\tilde{x}(t)-\tilde{x}(t-\sigma_p(t))-\int_{t-\sigma_p(t)}^{t}\dot{\tilde{x}}(s)ds\Big]=0, \tag{28}$$

being $G_{(l,\tau)}$, $G_{(p,\sigma)} \in \mathbb{R}^{2N\times 2N}$ $(\forall l=1,\dots,q\ p=1,\cdots,m)$ free matrices. Then, name $\rho(t,\tau_l(t),\sigma_p(t)) = [\tilde{x}(t-\tau_1(t))\ \cdots\ \tilde{x}(t-\tau_q(t))\ \tilde{x}(t-\sigma_1(t))\ \cdots\ \tilde{x}(t-\sigma_m(t))]^\top \in \mathbb{R}^{2(q+m)N\times 2(q+m)N}$, $\xi(t,\tau_l(t)\sigma_p(t)) = [\int_{t-\tau_1(t)}^{t}\tilde{x}(s)ds \cdots \int_{t-\tau_q(t)}^{t}\tilde{x}(s)\ \int_{t-\sigma_1(t)}^{t}\tilde{x}(s)ds \cdots \int_{t-\sigma_m(t)}^{t}\tilde{x}(s)ds]^\top \in \mathbb{R}^{2(q+m)N\times 2(q+m)N}$, $\varepsilon(t,\tau_l(t),\sigma_p(t)) = [\int_{t-\tau_1(t)}^{t}\dot{\tilde{x}}(s)ds \cdots \int_{t-\tau_q(t)}^{t}\dot{\tilde{x}}(s)\ \int_{t-\sigma_1(t)}^{t}\dot{\tilde{x}}(s)ds \cdots \int_{t-\sigma_m(t)}^{t}\dot{\tilde{x}}(s)ds]^\top \in \mathbb{R}^{2(q+m)N\times 2(q+m)N}$, and introduce the following augmented state vector: $\eta(t) = [\tilde{x}(t)\ \ \rho(t,\tau_l(t),\sigma_p(t))\ \ \xi(t,\tau_l(t),\sigma_p(t))\ \ \varepsilon(t,\tau_l(t),\sigma_p(t))]^\top \in \mathbb{R}^{\delta\times\delta}$ being $\delta = 2N[3(q+m)+1]$.

Accordingly, summing up (24)-(26) as well as the null terms (27)-(28), the following inequality is obtained:

$$\dot{V}(\tilde{x}(t)) \leq \eta^\top(t)\Theta\eta(t), \tag{29}$$

where $\Theta \in \mathbb{R}^{\delta\times\delta}$ is the following block matrix:

$$\begin{bmatrix}\Theta_{11} & 0^{2N\times 2(q+m)N} & 0^{2N\times 2(q+m)N} & \Theta_{14}\\ 0 & -\begin{bmatrix}\tilde{Q}_\tau & 0\\ 0 & \tilde{Q}_\sigma\end{bmatrix} & 0 & -\begin{bmatrix}\tilde{G}_\tau^\top & 0\\ 0 & \tilde{G}_\sigma^\top\end{bmatrix}\\ 0 & 0 & -\begin{bmatrix}\tilde{W}_\tau & 0\\ 0 & \tilde{W}_\sigma\end{bmatrix} & 0\\ 0 & 0 & 0 & -\begin{bmatrix}\tilde{G}_\tau & 0\\ 0 & \tilde{G}_\sigma\end{bmatrix}\end{bmatrix}, \tag{30}$$

being

$$\begin{aligned}\Theta_{11} =& \Big(\Phi+\sum_{l=1}^{q}Q_{(l,\tau)}+\sum_{p=1}^{m}Q_{(p,\sigma)}+(m+q)\tau^\star\Big(\sum_{l=1}^{q}W_{(l,\tau)}+\sum_{p=1}^{m}W_{(p,\sigma)}\Big)\Big),\\ \Theta_{14} =& [G_{(1,\tau)}-A_{(1,\tau)}\ \cdots\ G_{(q,\tau)}-A_{(q,\tau)}\ G_{(1,\sigma)}-A_{(1,\sigma)}\ \cdots\ G_{(m,\sigma)}-A_{(m,\sigma)}],\\ \tilde{Q}_\tau =& \operatorname{diag}(Q_{(1,\tau)}(1-\mu_1),\cdots,Q_{(q,\tau)}(1-\mu_q)),\\ \tilde{Q}_\sigma =& \operatorname{diag}(Q_{(1,\sigma)}(1-\mu_1),\cdots,Q_{(m,\sigma)}(1-\mu_m)),\\ \tilde{W}_\tau =& \operatorname{diag}(W_{(1,\tau)},\cdots,W_{(q,\tau)}), \qquad \tilde{W}_\sigma = \operatorname{diag}(W_{(1,\sigma)},\cdots,W_{(m,\sigma)}),\\ \tilde{G}_\tau =& \operatorname{diag}(G_{(1,\tau)},\cdots,G_{(q,\tau)}), \qquad \tilde{G}_\sigma = \operatorname{diag}(G_{(1,\sigma)},\cdots,G_{(m,\sigma)}).\end{aligned} \tag{31}$$

Hence, the asymptotic stability of the delayed closed-loop system in (13) is guaranteed if the matrix Θ in (30) is negative definite. Due to its structure, $\Theta < 0$ if each diagonal block matrix is negative definite. Taking into account Assumption 1, since $Q_{l,\tau}$, $Q_{p,\sigma}$, $W_{l,\tau}$, $W_{p,\sigma}$ are positive matrices while $G_{(l,\tau)}$, $G_{(p,\sigma)}$ are free matrices selected positive $(\forall l,p)$, it follows that $\Theta < 0$ if the LMI in (19) holds. ■

TABLE I: Heterogeneous Vehicles Dynamics Parameters.

Vehicle mass $[m_0,m_1,\dots,m_5]^\top$ $[Kg]$	$[1545, 1015, 1375, 1430, 1067, 1155]^\top$
Wheel radius $[R_0,R_1,\dots,R_5]^\top$ $[mm]$	$[306, 283, 288, 328, 265, 288]^\top$
Rolling resistance $[f_0,f_1,\dots,f_5]^\top$ $[-]$	$[0.020, 0.022, 0.019, 0.021, 0.023, 0.024]^\top$
Drag coefficient $[C_{D,0},C_{D,1},\dots,C_{D,5}]^\top$ $[-]$	$[0.3, 0.3, 0.24, 0.29, 0.29, 0.33]^\top$
Frontal area $[A_{f,0},A_{f,1},\dots,A_{f,5}]^\top$ $[m^2]$	$[2.2, 2.19, 2.4, 2.46, 2.14, 2.04]^\top$

Remark 1: Theorem 1 provides a delay-dependent stability criterion expressed as a set of LMIs that allows the proper tuning of the control gains in (9). LMI (19) can be numerically verified by using the Yalmip Toolbox [14].

V. Simulation Analysis

This section investigates the effectiveness of the proposed control approach in guaranteeing platoon formation under the proposed nonlinear spacing policy via MiTraS simulation platform [13]. We consider a heterogeneous platoon composed of $N = 5$ CAVs (with equal length of $4.7[m]$ and $\eta_i = 0.89$, $\forall i = 1,\cdots,N$), plus the leader following a trapezoidal speed profile. The initial conditions are $[p_0(0), p_1(0),\dots,p_5(0)] = [280, 250.3, 220.6, 190.9, 161.2, 131.5][m]$ and $v_i(0) = 18[m/s]$ $(\forall i = 0,1,\cdots,N)$, while CAVs parameters are listed in Table I. The connectivity among vehicles undergoes Leader-Predecessor-Follower (LPF) topology while communication delays are emulated as random variable uniformly distributed within the range $[0, 0.05]$ $[s]$. Accordingly, the control gains in (9) are selected via Theorem 1 as: $[\kappa_{10},\ \kappa_{20},\ \kappa_{21},\ \kappa_{30},\ \kappa_{32},\ \kappa_{40},\ \kappa_{43},\ \kappa_{50},\ \kappa_{54},] = [318,\ 143,\ 135,\ 149,\ 120,\ 149,\ 120,\ 110,\ 120]$ and $[\beta_{10},\ \beta_{20},\ \beta_{21},\ \beta_{30},\ \beta_{32},\ \beta_{40},\ \beta_{43},\ \beta_{50},\ \beta_{54}] = [393,\ 177,\ 80,\ 185,\ 80,\ 138,\ 80,\ 149,\ 80]$. Results in Fig.s 2 (a) and (b) depict the inter-vehicle distance and speed profiles of CAVs platoon and disclose how formation control objectives (6) are achieved. Indeed, the proposed strategy ensures that each vehicle tracks the leader speed profile with smooth behaviour during transient phases and without over-shoots and under-shoots, while maintaining the variable nonlinear spacing policy $d_{ref,ij}(t)$ $((i,j) \in \mathscr{E}_{N+1})$. Fig. 2$(c)$ compares the proposed nonlinear spacing with the typical CTG when $h = 0.6$ and $h = 0.9$. As expected, the behaviour of the proposed policy is comparable to $CTG_{h=0.6}$ for low speed, while it ensures larger (and safer) distance at higher speed (but still significantly lower than $CTG_{h=0.9}$). This further confirms how the proposed spacing is able to guarantee an increasing of traffic throughput, differently from $CTG_{h=0.9}$ while ensuring the vehicles safety at high speed, differently from $CTG_{h=0.6}$ (see also Figure 1). To capture variations in longitudinal vehicles control, we also calculate Driving Volatility [21] index with a 3 seconds-time window. The results listed in Table II highlight that the proposed spacing policy significantly reduces the speed variation w.r.t. $CTG_{h=0.6}$ with a behavior comparable to $CTG_{h=0.9}$ despite lower inter-vehicle distances.

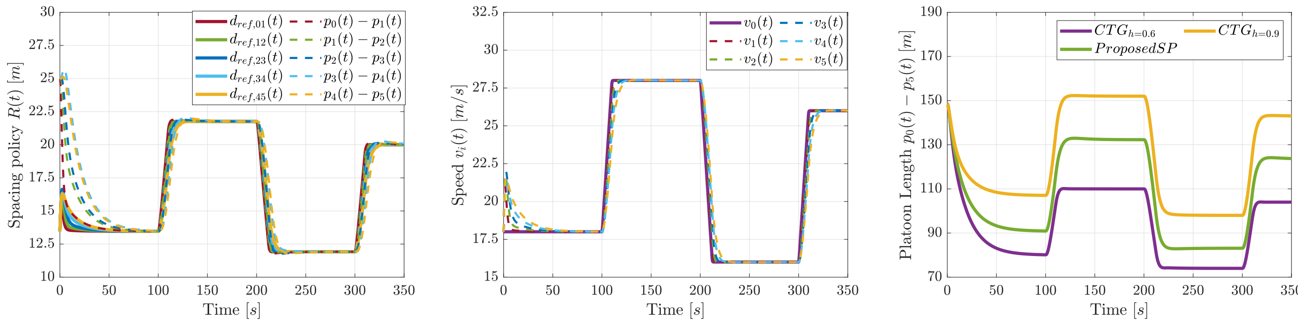

(a) (b) (c)

Fig. 2: Platoon formation control under (9): (a) Time history of the desired spacing policy between consecutive vehicles, i.e. $d_{ref,ii-1}(t)$ (see solid lines), vs the actual inter-vehicle distance $p_{i-1}(t)-p_i(t)$ (see dashed lines), $\forall i=1,\cdots,N$; (b) Time history of vehicles speed $v_i(t)$ $\forall i=0,1,\ldots,N$; (c) Time history of platoon length when comparing (4) with respect to $CTG_{h=0.6}$ and $CTG_{h=0.9}$.

TABLE II: Comparison w.r.t. different spacing policy implementation: Driving Volatility value $[m/s]$ and improvement percentage.

Spacing Policy	Vehicle 1	Vehicle 2	Vehicle 3	Vehicle 4	Vehicle 5
Proposed (4)	52.6	54.6	55.7	55.2	55.2
$CTG_{h=0.6}$	56.0 -6.1%	60.0 -9%	60.5 -8%	58.0 -4.9%	57.4 -3.9%
$CTG_{h=0.9}$	52.4 $+0.3\%$	54.1 $+0.9\%$	53.6 +3,9%	52.9 +4,3%	52.7 +4,7%

VI. Conclusions

This paper has addressed the platoon control problem for nonlinear CAVs, sharing information via a non ideal V2V network, under nonlinear variable spacing policy. After suggesting a variable time-gap based desired inter-vehicle distance, covering the full speed range for platooning control systems, the problem is recast as a formation control one. Thus, a distributed robust control strategy is proposed to ensure that each CAV in the platoon tracks the desired motion while maintaining the desired variable spacing policy, adapted to the current traffic situation, despite the presence of communication impairments. Simulation analysis disclose the effectiveness and the advantages of the proposed solution.

References

[1] Q. Li, Z. Chen, and X. Li, "A review of connected and automated vehicle platoon merging and splitting operations," *IEEE Transactions on Intelligent Transportation Systems*, 2022.

[2] M. Čičić, C. Pasquale, S. Siri, S. Sacone, and K. H. Johansson, "Platoon-actuated variable area mainstream traffic control for bottleneck decongestion," *European Journal of Control*, vol. 68, p. 100687, 2022.

[3] C. Wu, Z. Xu, Y. Liu, C. Fu, K. Li, and M. Hu, "Spacing policies for adaptive cruise control: A survey," *IEEE Access*, vol. 8, pp. 50 149–50 162, 2020.

[4] S. Siri, C. Pasquale, S. Sacone, and A. Ferrara, "Freeway traffic control: A survey," *Automatica*, vol. 130, p. 109655, 2021.

[5] P. Wijnbergen, M. Jeeninga, and B. Besselink, "Nonlinear spacing policies for vehicle platoons: A geometric approach to decentralized control," *Systems & Control Letters*, vol. 153, p. 104954, 2021.

[6] G. Guo, P. Li, and L.-Y. Hao, "Adaptive fault-tolerant control of platoons with guaranteed traffic flow stability," *IEEE Transactions on Vehicular Technology*, vol. 69, no. 7, pp. 6916–6927, 2020.

[7] J. Chen, H. Liang, J. Li, and Z. Lv, "Connected automated vehicle platoon control with input saturation and variable time headway strategy," *IEEE Transactions on Intelligent Transportation Systems*, vol. 22, no. 8, pp. 4929–4940, 2020.

[8] J. Zhou and H. Peng, "Range policy of adaptive cruise control vehicles for improved flow stability and string stability," *IEEE Transactions on intelligent transportation systems*, vol. 6, no. 2, pp. 229–237, 2005.

[9] L. Zuo, P. Wang, M. Yan, and X. Zhu, "Platoon tracking control with road-friction based spacing policy for nonlinear vehicles," *IEEE Transactions on Intelligent Transportation Systems*, vol. 23, no. 11, pp. 20 810–20 819, 2022.

[10] L. Shao, C. Jin, C. Lex, and A. Eichberger, "Robust road friction estimation during vehicle steering," *Vehicle system dynamics*, vol. 57, no. 4, pp. 493–519, 2019.

[11] Y. Li, Q. Lv, H. Zhu, H. Li, H. Li, S. Hu, S. Yu, and Y. Wang, "Variable time headway policy based platoon control for heterogeneous connected vehicles with external disturbances," *IEEE Transactions on Intelligent Transportation Systems*, vol. 23, no. 11, pp. 21 190–21 200, 2022.

[12] C. Flores, V. Milanés, and F. Nashashibi, "A time gap-based spacing policy for full-range car-following," in *2017 IEEE 20th International Conference on Intelligent Transportation Systems (ITSC)*. IEEE, 2017, pp. 1–6.

[13] G. N. Bifulco, A. Coppola, A. Petrillo, and S. Santini, "Decentralized cooperative crossing at unsignalized intersections via vehicle-to-vehicle communication in mixed traffic flows," *Journal of Intelligent Transportation Systems*, pp. 1–26, 2022.

[14] A. Coppola, D. G. Lui, A. Petrillo, and S. Santini, "Eco-driving control architecture for platoons of uncertain heterogeneous nonlinear connected autonomous electric vehicles," *IEEE Transactions on Intelligent Transportation Systems*, vol. 23, no. 12, pp. 24 220–24 234, 2022.

[15] E. Fridman, "Tutorial on lyapunov-based methods for time-delay systems," *European Journal of Control*, vol. 20, no. 6, pp. 271–283, 2014.

[16] A. Coppola, D. G. Lui, A. Petrillo, and S. Santini, "Cooperative driving of heterogeneous uncertain nonlinear connected and autonomous vehicles via distributed switching robust pid-like control," *Information Sciences*, vol. 625, pp. 277–298, 2023.

[17] H. E. Sungu, M. Inoue, and J.-i. Imura, "Nonlinear spacing policy based vehicle platoon control for local string stability and global traffic flow stability," in *2015 European Control Conference (ECC)*. IEEE, 2015, pp. 3396–3401.

[18] A. Petrillo, A. Salvi, S. Santini, and A. S. Valente, "Adaptive multi-agents synchronization for collaborative driving of autonomous vehicles with multiple communication delays," *Transportation research part C: emerging technologies*, vol. 86, pp. 372–392, 2018.

[19] S. Manfredi, A. Petrillo, and S. Santini, "Distributed pi control for heterogeneous nonlinear platoon of autonomous connected vehicles," *IFAC-PapersOnLine*, vol. 53, no. 2, pp. 15 229–15 234, 2020.

[20] Y. He, M. Wu, J.-H. She, and G.-P. Liu, "Delay-dependent robust stability criteria for uncertain neutral systems with mixed delays," *Systems & Control Letters*, vol. 51, no. 1, pp. 57–65, 2004.

[21] I. Mahdinia, R. Arvin, A. J. Khattak, and A. Ghiasi, "Safety, energy, and emissions impacts of adaptive cruise control and cooperative adaptive cruise control," *Transportation Research Record*, vol. 2674, no. 6, pp. 253–267, 2020.